ELSEVIER

3 December 2001

Physics Letters A 291 (2001) 115–123

PHYSICS LETTERS A

www.elsevier.com/locate/pla

Simultaneous existence of a multiplicity of stable and unstable solitons in dissipative systems

J.M. Soto-Crespo [a,*], Nail Akhmediev [b,c], Kin S. Chiang [c]

[a] *Instituto de Óptica, CSIC, Serrano 121, 28006 Madrid, Spain*

[b] *Australian Photonics CRC, Optical Science Centre, Research School of Physics Science and Engineering, Australian National University, Canberra ACT 0200, Australia*

[c] *Department of Electronic Engineering, City University of Hong Kong, Hong Kong*

Received 10 July 2001; accepted 26 September 2001
Communicated by A.R. Bishop

Abstract

We show that dissipative systems can have a multiplicity of stationary solutions in the form of both stable and unstable solitons. As a model equation, we use the complex cubic–quintic Ginzburg–Landau equation. For a given set of the equation parameters, this equation has many coexisting soliton solutions. Our stability results show that although most of them are unstable, they can have stable pieces. This partial stability leads to the phenomenon of soliton explosion. © 2001 Elsevier Science B.V. All rights reserved.

PACS: 42.65
Keywords: Ginzburg–Landau equation; Solitons; Dissipative systems

1. Introduction

The emergence of stable spatio-temporal patterns in a variety of physical situations may be modeled through the well-known complex Ginzburg–Landau equation (CGLE). These include a variety of nonequilibrium phenomena, such as the dynamics of certain chemical reactions [1], binary fluid convection [2], soliton propagation in optical fiber systems with linear and nonlinear gain and spectral filtering (such as communication links with lumped fast saturable absorbers [3–7] or pulse generation in fiber lasers with additive-pulse mode-locking or nonlinear polarization rotation [8–14]). In two transverse dimensions, the variety of patterns shows many possible ways, towards which the system can evolve [15–19]. However, the explanation of all these patterns in two dimensions might be complicated.

In fact, even in one dimension, localized structures in dissipative systems come out in multiplicity. Similar phenomenon is known for solitons in Hamiltonian systems [20]. However, there is a significant difference between solitons in Hamiltonian and dissipative systems. In Hamiltonian systems, soliton solutions appear as a result of a balance between diffraction (dispersion) and nonlinearity. Diffraction spreads the beam while nonlinearity focuses it and makes it narrower. The balance between the two opposed effects results in stationary solutions, which are usually a one-parameter family. In systems with gain and loss,

* Corresponding author.
E-mail address: iodsc09@io.cfmac.csic.es (J.M. Soto-Crespo).

PII: S0375-9601(01)00634-X

in order to have stationary solutions, gain and loss must also be balanced. This additional balance results in solutions which are fixed. The shape, amplitude and the width are all fixed and depend on the parameters of the equation. There can be exceptions to this rule [21–23], but, usually, the solutions are fixed (i.e., isolated from each other). On the other hand, the number of fixed solutions which exist for the same set of parameters of the system can be more than one. In some cases, we can observe simultaneously up to five stable solutions [24]. Usually each type of solution is stable for a certain region in the space of parameters, which can overlap in a narrower region resulting in multistability.

Let us also recall that the range of existence for dissipative solitons has a different meaning from that for solitons in Hamiltonian systems. Dissipative solitons are fixed solutions and the range of existence can only be defined in the space of the equation parameters. In Hamiltonian systems, stationary solutions have free parameters not directly related to the parameters of the equation. Consequently, the range of soliton existence in Hamiltonian systems is in a different space: in the space of the parameters of the solution.

In addition to stable solutions, there can be unstable ones which are "invisible" if we are interested only in stable structures and look for them by solving the whole propagation equation [24,25]. However, those might play an essential role in the overall dynamics when the system starts with an arbitrary initial condition. Moreover, some solutions when continued in the space of system parameters have different stability properties over the total region of their existence. Hence, changing the parameters of the system we can switch patterns observed in this system. Another phenomenon which we discovered in this work is that the same soliton can be partly stable and partly unstable. An example of complicated dynamics which might be caused by such stable–unstable "modes" is a "exploding" soliton [26]. The conclusion is that both types of stationary solitons stable and unstable are important and deserve careful study.

In the situation where a single transverse coordinate is retained in the analysis, the CGLE reads as [20]

$$i\psi_z + \frac{D}{2}\psi_{tt} + |\psi|^2\psi = i\delta\psi + i\epsilon|\psi|^2\psi + i\beta\psi_{tt} + i\mu|\psi|^4\psi - \nu|\psi|^4\psi, \tag{1}$$

where D, δ, β, ϵ, μ, and ν are real constants (we do not require them to be small), and ψ is a complex field. By a proper rescaling and without loss of generality D can be restricted to have the values $D = \pm 1$.

The CGLE applies, for example, to describing propagation of light in an active dispersive medium (e.g., a doped optical fiber). In this case, t is a retarded time, z is the propagation distance, ψ is the complex envelope of the electric field, D is the dispersion (diffraction) coefficient, δ gives account of the linear gain, β describes spectral filtering or parabolic gain ($\beta > 0$), ϵ accounts for nonlinear gain/absorption processes, μ represents a higher-order correction to the nonlinear amplification/absorption, and ν is a possible higher-order correction term to the intensity-dependent refractive index.

The cubic–quintic CGLE was considered in a number of publications using numerical simulations, perturbative analysis and analytic solutions. Perturbative analysis of the solitons of the quintic CGLE in the NLSE limit (i.e., for the anomalous dispersion regime) was developed in [27,28]. The existence of soliton-like solutions of the quintic CGLE in the case of subcritical bifurcations ($\epsilon > 0$) was also numerically determined [28,29]. More recently, the regions in the parameter space at which stable pulse-like solutions exist were found for the case of anomalous [30] and normal dispersion [31]. A qualitative analysis of the transformation of the regions of existence of the pulse-like solutions, when the coefficients on the right-hand side change from zero to infinity, was done in [27]. An analytic approach, based on the reduction of Eq. (1) to a three-variable dynamical system, which allows to obtain exact solutions for the quintic equation, was developed in [21].

Some analytic soliton solutions to this equation in the form of stationary pulses are known [22]. They exist only for a certain relation between the parameters and most of them are unstable [30]. Hence, numerical studies are unavoidable. Moreover, numerical studies give more branches of solitons than analytical expressions. The knowledge of their existence is very important because each stationary solution is a singular point in the infinite-dimensional phase space of the system and plays a certain role in the complicated and rich pulse dynamics.

In the present work, we are interested in the whole set of soliton solutions which include both stable and

unstable solitons existing for the same set of values of the equation parameters. We have found a multiplicity of solutions indeed, and studied numerically their stability properties over the range of their existence. The study of the unstable soliton dynamics revealed their new striking features.

2. Numerical technique

Exact analytical solutions can be found only for certain combinations of the values of the parameters [22]. In general we need to use some numerical technique to find stationary solutions. One way to do it is by reducing Eq. (1) to a set of ODEs. We do that by seeking solutions in the form

$$\begin{aligned}\psi(t,z) &= \psi_0(\tau)\exp(-i\omega z)\\ &= a(\tau)\exp\bigl[i\phi(\tau)-i\omega z\bigr],\end{aligned} \tag{2}$$

where a and ϕ are real functions of $\tau = t - vz$, v is the pulse velocity and ω is the nonlinear shift of the propagation constant. Substituting (2) into (1), we obtain an equation for two coupled functions, a and ϕ. Separating real and imaginary parts, after simple algebraic transformations, we get the following set of two ODEs:

$$\begin{aligned}&\omega a + v\frac{M}{a} - \frac{DM^2}{2a^3} + \frac{\beta M'}{a} + \frac{D}{2}a'' + a^3 + \nu a^5 = 0,\\ &-\delta a - va' + \frac{\beta M^2}{a^3} + \frac{DM'}{2a} - \beta a'' - \epsilon a^3 - \mu a^5\\ &\quad = 0,\end{aligned} \tag{3}$$

where $M = a^2\phi'$ and each prime denotes a derivative with respect to τ.

Separating derivatives, and looking only for zero-velocity ($v = 0$) solutions, we obtain

$$\begin{aligned}M' &= \frac{2(D\delta - 2\beta\omega)}{1+4\beta^2}a^2 + \frac{2(D\epsilon - 2\beta)}{1+4\beta^2}a^4\\ &\quad + \frac{2(D\mu - 2\beta\nu)}{1+4\beta^2}a^6,\\ a'' &= \frac{M^2}{a^3} - \frac{2(D\omega + 2\beta\delta)}{1+4\beta^2}a - \frac{2(D + 2\beta\epsilon)}{1+4\beta^2}a^3\\ &\quad - \frac{2(D\nu + 2\beta\mu)}{1+4\beta^2}a^5.\end{aligned} \tag{4}$$

This set of ODEs can be solved numerically. For localized solutions with correctly chosen ω, the amplitude a should go exponentially to zero outside the region of localization.

The asymptotic behavior of (4) at small a is given by $a = a_0\exp(g\tau)$ and $M = [(D\delta - 2\beta\omega)/g(1+4\beta^2)]a_0^2\exp(2g\tau)$, where a_0 is an arbitrary small amplitude and the soliton tail exponent g is given by

$$g^2 = \pm\sqrt{\frac{\omega^2+\delta^2}{1+4\beta^2}} - \frac{D\omega + 2\beta\delta}{1+4\beta^2}.$$

Then, adjusting properly ω, it is possible to find the rest of the pulse solution with a shooting method.

3. Multiplicity of solutions

Using the method described in Section 2, we have found that for a given set of values of the parameters, a number of stationary bounded solutions coexist simultaneously. The choice of parameters is somehow arbitrary. However, the phenomenon of the multiplicity of solutions is general and happens for almost any values of the parameters where we looked for them. We recall, in this respect, that even analytic solutions when they do exist, appear in pairs [22,31]. We restrict ourselves to zero velocity solitons. Otherwise the number of solutions would be much higher.

Fig. 1 illustrates the phenomenon of soliton multiplicity. It shows eight different soliton solutions found for the following values of the parameters: $D = +1$, $\delta = -0.1$, $\beta = 0.18$, $\epsilon = 1.5$, $\nu = -0.6$ and $\mu = -0.1$. In the rest of the Letter we always use this set of the equation parameters except for ϵ. We have separated the solutions into two sets, corresponding to (a) high- and (b) low-amplitude solutions (note the two different x- and y-scales). In each case there exists one plain soliton solution (solid line) and a multiplicity of composite and multipeak solutions.

Some of the high-peak-amplitude solutions have been previously discovered in [24,25]. They were named SP (single pulse), CP (composite pulse) and NCP (new composite pulse) and we keep the same notation here. Each of these solutions was reported to be stable for some range of the parameters. Moreover, it was also found that more than one of them (two or even three) can be stable simultaneously. The wider solution had not been previously known, we call it here NNCP (next new composite pulse). For the sake

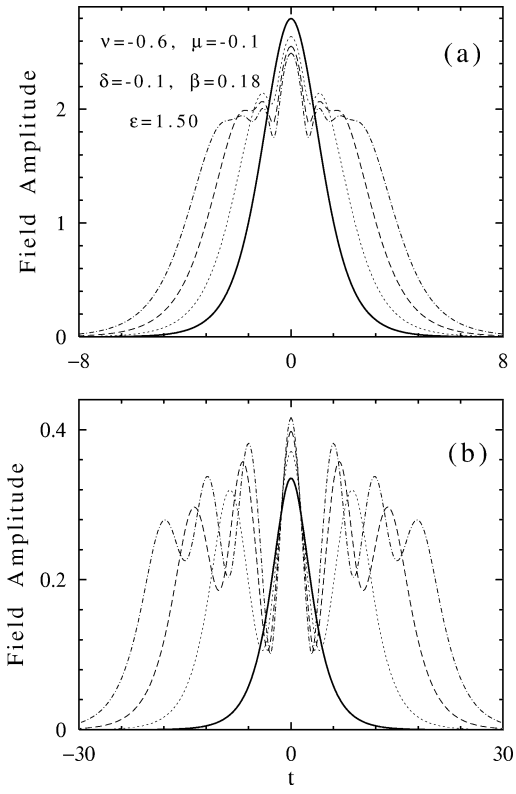

Fig. 1. Amplitude profile of eight stationary solutions for the same equation parameters. They are classified in the two categories: (a) High-amplitude solitons named SP (solid line), CP (dotted line), NCP (dashed line) and NNCP (dash-dotted line). (b) Low-amplitude solitons.

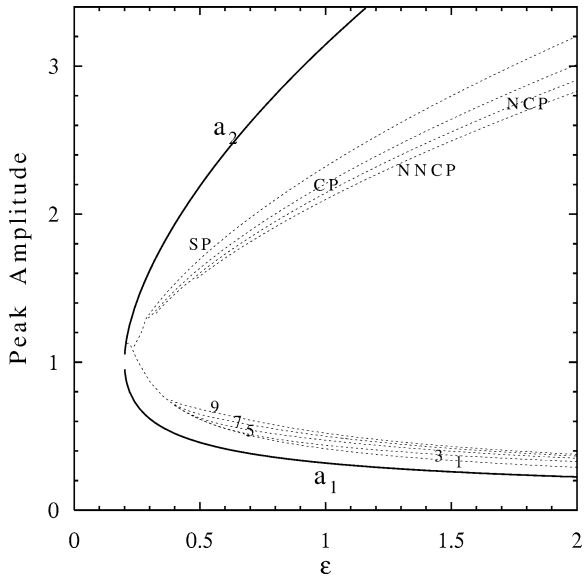

Fig. 2. Maximum soliton amplitude versus ϵ. Each curve represents a branch of soliton. It is labeled either with the given name or with the number of peaks it has. An example of each soliton at $\epsilon = 1.5$ is given in Fig. 1. The solid lines show the amplitudes a_1 and a_2 of the two CW solutions.

of clarity we show in Fig. 1 eight stationary solutions but there are more with increasing number of peaks. Besides, more localized stationary solutions could have been obtained if we had not imposed that $v = 0$ [24,25,32].

The soliton is defined uniquely if we know the value of its peak amplitude ($a(0)$) and its nonlinear shift of the propagation constant (ω). Any of these values can be used to classify the solutions. As we continuously change some of the equation parameters, each solution and its profile, in particular, continuously changes until it ceases to exist. Each type of solitons comprise a separate branch. We can represent these branches graphically plotting one of the soliton characteristics versus one of the equation parameters. Each branch on these plots will have its own range of existence.

Fig. 2 shows the amplitude at the soliton center (which is also the peak amplitude) versus ϵ for the solutions shown in Fig. 1. Additionally, Fig. 2 contains the curve corresponding to the 9-peak solution which is not shown in Fig. 1 but it has a structure similar to other solutions in Fig. 1. Each curve is labeled either with the name of the solution (e.g., SP, CP, NCP and NNCP for high-amplitude solutions) or with the number of peaks the solution has (for low-amplitude solutions). The amplitudes for the two classes of solutions change differently when ϵ changes. In the case of high-amplitude solitons, they monotonically increase as ϵ increases and the opposite happens for the low-amplitude set of solutions. Fig. 2 shows also the values a_1 and a_2 for the amplitudes of the two continuous wave (CW) solutions of Eq. (1). Each of the high- and low-amplitude soliton solutions have its analog in the form of the CW with high and low amplitude. Moreover, all soliton amplitudes are contained between these two lines. The analysis also shows that there is a minimum value of ϵ for the existence of solitons and plane wave solutions. This minimum is dictated by the requirement of having sufficient counterbalance to linear (δ) and quintic (μ) losses in the equa-

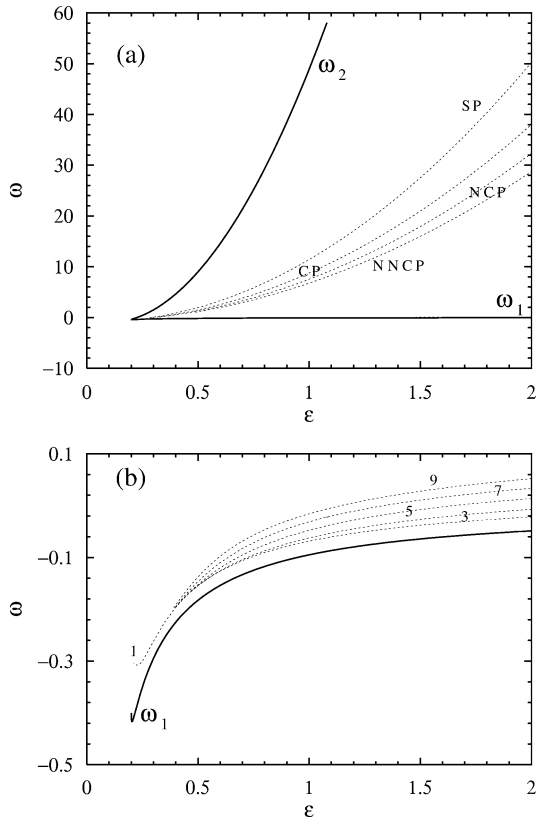

Fig. 3. (a) Propagation constant ω versus ϵ for same branches of solitons as in Fig. 2 and for CW solutions. (b) A part of (a) in magnified scale.

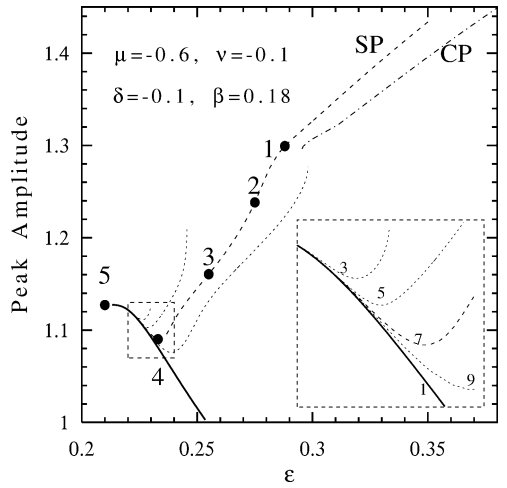

Fig. 4. The maximum amplitude of the soliton solution versus ϵ. This is a zoomed part of Fig. 2. The filled circles correspond to solutions shown in Fig. 5. The inset in the right bottom corner shows a magnification of the part of the figure enclosed in a dashed line rectangle.

tion. If the cubic gain ϵ is smaller than the threshold $2\sqrt{\mu\delta}$, any solution will eventually disappear.

The nonlinear propagation constant ω versus ϵ for all soliton solutions is shown in Fig. 3. In addition, the curves ω versus ϵ for the two CW solutions (ω_1 and ω_2) are also shown in Fig. 3(a). It can be seen that the curves for soliton solutions are located in between the ω values for CW solutions. With the chosen vertical scale the curves for ω_1 and the low-amplitude solutions are indistinguishable. To show the separation clearly, in Fig. 3(b) we magnified the part corresponding to these solutions.

In principle, the curves for the peak amplitude versus ϵ could cross each other. If this happens, the points which belong to different curves represent different solutions at the intersection point as the value ω for them would be different. However, this does not happen in the case of the curves shown in Fig. 2. As two curves ($a(0)$ versus ϵ) approach each other, their respective ω values also get closer to each other. The soliton at the edge of a branch is transformed into the soliton of another branch.

In the case of the low-amplitude solutions with several peaks, as we decrease ϵ, the peaks move away from each other, until they are transformed into separated plain solitons with identical profiles but with certain phase difference [32,33] between consecutive peaks. The interaction through their tails weakens and in the limit each peak can be considered as a separate soliton. Hence, the curves corresponding to these solutions asymptotically merge with the curve for the plain solitons of low amplitude. This can be clearly seen in Figs. 2 and 3(b).

Splitting phenomenon also happens with the SP solitons. Fig. 4 is a magnification of a part of Fig. 2. The inset shows a further magnification of that part in Fig. 4 which is enclosed in a dashed rectangle. Additional curves corresponding to N-peak soliton solutions are shown by dotted lines ($N = 3, 5, 9$). The labels in the inset denote the number of peaks in the soliton profile.

The curve for plain solitons with higher amplitude (SP) asymptotically converges to the curve for plain

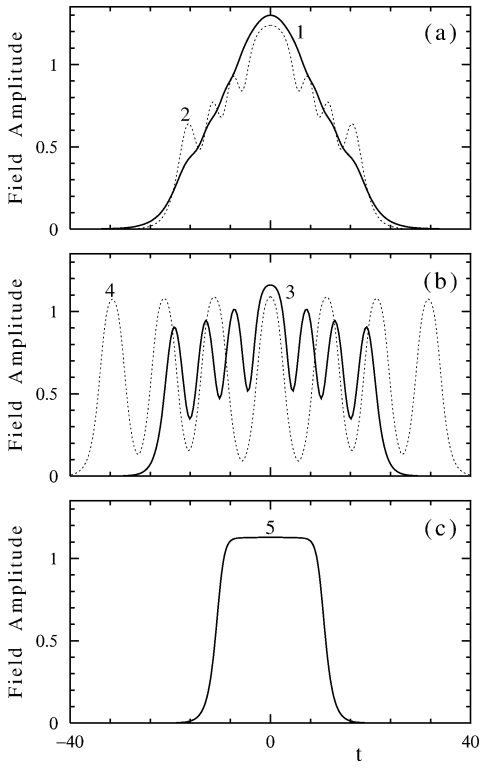

Fig. 5. Amplitude profiles of the stationary solutions marked in Fig. 4 by filled circles with the same labels. The values of the parameters are $\delta = -0.1$, $\beta = 0.18$, $\mu = -0.1$, $\nu = -0.6$, and (a) $\epsilon = 0.288$ (curve 1, solid line), 0.275 (curve 2, dotted line), (b) 0.255 (curve 3, solid line), 0.233 (curve 4, dotted line), (c) 0.210 (flat top soliton).

low-amplitude solutions. Reducing ϵ causes a weak modulation of the profile of the SP solution. The modulation depth grows creating 7-peak solutions and at even lower ϵ it transforms into 7 separate solitons weakly interacting through their tails. The appearance of the modulation in the soliton profile causes the increase of the amplitude of each peak. The curves go up when ϵ decreases. This process is clearly visible in the Fig. 4. The same happens to the 3-, 5- and 9-peak solutions: their corresponding soliton branches converge to the curve for the low-amplitude plain solutions. At the same time they become transformed into N-soliton solutions ($N = 3, 5, 9$).

This transformation is illustrated in Fig. 5, which shows five profiles corresponding to the solutions marked with a filled circles in Fig. 4 labeled in the same way. The value of the parameters is written in the caption. In Fig. 5(a) the modulation of profile (1) is hardly visible while it is more developed and has a multipeak structure in profile (2). Fig. 5(b) shows how the seven peaks grow and gradually separate from each other (3). Decreasing ϵ a little more transforms the solution into seven plain solitons interacting only through their tails as in the case of curve (4). Further decrease of ϵ separates completely these seven solitons and ceases their interaction. For smaller ϵ, each single pulse changes its profile continuously towards a flat-top soliton as shown in Fig. 5(c).

4. Stability analysis and soliton evolution

In general, the stability of the soliton solutions is an open question. Stability of solitons in the limit of nonlinear Schrödinger equation, i.e., when the coefficients at the right-hand side of Eq. (1) are small, has been analyzed in Ref. [34]. We are interested in the case of arbitrary values of these coefficients. At this stage we do not have a general stability criterion for dissipative solitons. Our experience shows that several branches of solitons can be stable simultaneously [24, 25]. To shed some light on this issue, we performed a linear stability analysis [30] of the above described solutions. It allowed us to obtain the perturbation with the largest growth rate and its corresponding eigenvalue g. This growth rate is shown in Fig. 6. Each curve is labeled with the name of the soliton branch we used above.

In the interval of values of ϵ under study (0.2–2.0), the growth rate associated to the composite solitons (CP, NCP and NNCP) is usually more than an order of magnitude higher than those of the other solitons, so we plotted them in two different scales in Figs. 6(a) and (b). In order to compare these values with the corresponding growth rates for the SP solitons, in Fig. 6(b) we use a logarithmic scale along the vertical axis.

For all soliton branches, the growth rate increases with ϵ. An exception is the branch of SP solitons. Almost at the whole range of ϵ SP solitons have the smallest growth rate and for ϵ greater than 1.40 the SP solitons are stable. Hence, in the range of interest, only SP solitons can be stable and this happens at $\epsilon > 1.4$.

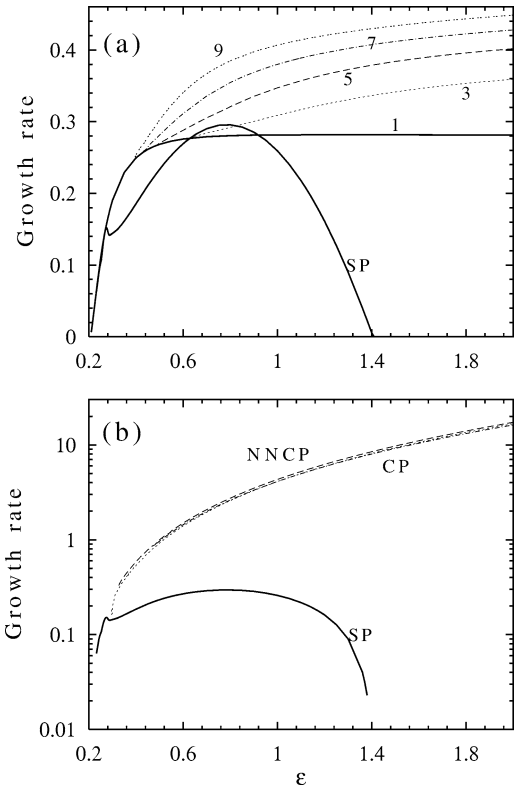

Fig. 6. Growth rates of perturbation versus ϵ for (a) low-amplitude and SP solitons (in linear scale) and (b) the composite and SP solitons (in logarithmic scale). The labels 1, 3, 5, 7, 9 in (a) refer to the number of peaks in the low-amplitude soliton profiles.

An important fact is that in general the eigenvalue, g, for the SP solitons is complex and has both real and imaginary parts. This is what we would expect for dissipative solitons. The imaginary part is not shown in the plots. On the other hand, all composite solitons, namely CP, NCP and NNCP, have purely real eigenvalues. Moreover, the values of the growth rate for these three branches are very close to each other as we can see from Fig. 6(b).

An example of perturbation function with the largest growth rate for SP soliton is shown in Fig. 7. Its corresponding eigenvalue is $g = 0.297 + i6.72$. The perturbation function is mainly nonzero at the slopes of the soliton and is almost zero around the top of the soliton. Hence, on propagation, the tails of the soliton are the first to experience changes whilst the center of the pulse will remain stationary for longer distances.

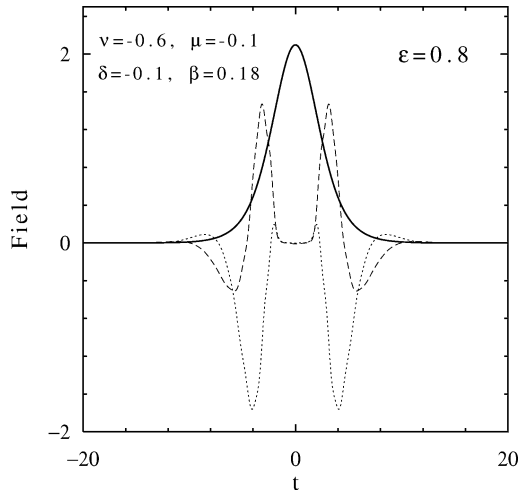

Fig. 7. Real (dotted line) and imaginary (dashed line) parts of the perturbation function for the SP soliton with $\epsilon = 0.8$. The solid line shows the amplitude of the SP soliton itself.

We have simulated the propagation of stationary solutions belonging to various branches of solitons. In absence of perturbations all solutions which are presented in previous sections can propagate long distances without visible changes confirming the fact that they are stationary solutions. Changes occur only when the accumulated numerical error becomes big enough to perturb the exact solution. However, if we apply a finite initial perturbation to the solution it will increase exponentially with z and reshape the solution quickly. The perturbation can be taken with either negative or positive sign. The choice of this sign plays the major role in the reshaping process.

The initial condition we used is $\psi(0,t) = \psi_0(t) \pm 0.001 f(t)$, where $f(t)$ is the perturbation function with the largest growth rate as calculated in the previous section, normalized to have the same norm as the stationary solution $\psi_0(t)$. The evolution will not change significantly if, instead, we add any other localized function to $\psi_0(t)$ not orthogonal to $f(t)$.

Due to the instability any stationary solution tends, generally speaking, to degrade. Low-amplitude solutions lose energy and gradually vanish if the initial perturbation is negative. If the perturbation is positive, the solution gains energy and transforms itself into a SP soliton.

The unstable solitons with higher energy after the degradation are transformed into the SP solution of the

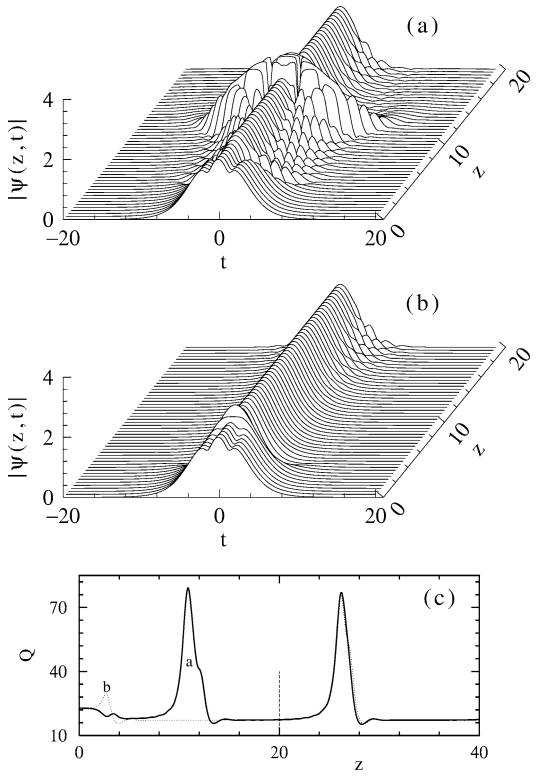

Fig. 8. Evolution of a CP soliton initially disturbed by (a) adding or (b) subtracting its perturbation function with the largest growth rate. Evolution of the energy, Q, at longer distance z for the cases (a) (solid line) and (b) (dotted line) is shown in (c). The vertical dashed line in (c) marks the value of z where simulations are stopped at (a) and (b).

stable branch when $\epsilon > 1.4$. This scenario would be expected from our stability analysis. The unusual part is that the solution converges to the SP soliton even when it is unstable, i.e., when ϵ is below 1.4. Fig. 8 shows what happens when the unstable CP soliton for $\epsilon = 0.8$ evolves in z. The instability transforms the CP into a SP. However, the SP soliton is also unstable and it exists for a limited distance z. Then SP develops instability around the tails which grow and simultaneously oscillate. Oscillations are expected because the perturbation function has a complex eigenvalue with both real and imaginary parts different from zero.

Depending on the sign of the perturbation function the side peaks increase or decrease their size while the central peak changes towards the profile of a SP soliton. In the case of positive perturbation (Fig. 8(a)) the shape becomes highly modulated leading quickly to an explosion. In the case of negative perturbation (Fig. 8(b)), the solution is transformed into a very neat SP soliton. In either case, oscillations appear sooner or later in the tails. Their amplitude grows exponentially. Finally, the SP soliton "explodes": it cracks into many pieces that eventually die out but a new SP solution appears from the pieces of this explosion. The process repeats indefinitely [26]. Fig. 8(c) shows the evolution of the energy $Q = \int_{-\infty}^{\infty} |\psi(z,t)|^2\,dt$ up to $z = 40$. It shows the second "explosion" at larger z for case (a) and the first for case (b), which casually almost coincide at the same z.

Very similar process is observed when the input is an NCP or an NNCP soliton. When ϵ increases approaching to the threshold of the instability, the distance between explosions increases and when ϵ is near the threshold, the modulation appears but does not produce an explosion. The eigenvalue of the perturbation becomes purely imaginary. The result of evolution is a perfectly periodic solution. The central peak of the soliton does not change but the tails oscillate with fixed amplitude.

An interesting result of our investigation is that the SP soliton is "stable" even if the growth rate of the instability has positive real part, i.e., below $\epsilon = 1.4$, although in a very peculiar way. The soliton keeps exploding but returns to the original shape periodically in z. The explanation for this strange behavior can be found in Fig. 7. The perturbation function effectively divides the soliton into three parts as if it would consist of three objects: the top of the soliton and two fronts, in the same way as CP solitons. Apparently, the two wings at these values of parameters are unstable but the top of the soliton is stable as the perturbation function is zero here. On propagation, the tails of the SP soliton are subject to shape transformation in contrast to the top of the soliton which survives these transformations. The solution have a chance to converge to this soliton which has at least a stable central part.

We recall, in this respect, that higher-order solitons in $(2+1)$-dimensional Hamiltonian systems can also be unstable in parts. Namely, the perturbation function for these solutions is nonzero mostly at the location of the rings that surround the central beam of the soliton [35]. As a result, the rings are unstable and split into separate filaments on evolution. The central

part of the higher-order soliton in this description remains "stable". This "partial stability" cannot happen to ground state solitons of Hamiltonian systems. In dissipative systems, as we can see, even the "fundamental" soliton can be unstable in parts.

5. Conclusion

In conclusion, we found a plethora of soliton solutions of the quintic CGLE. Namely, we obtained various types of composite solitons and multipeaked localized structures. We studied the interval of values of ϵ where they exist, at fixed values of δ, β, μ and ν. In this way we have found different branches of solitons and studied the splitting of these branches. We have studied the soliton stability using linearized equations and verified our predictions by solving the original CGLE. We have found that some solutions can be stable in parts and this partial stability might serve as a key to understand the unusual behavior of the "exploding" solitons.

Acknowledgements

The work of J.M.S.C. was supported by the Dirección General de Enseñanza Superior under contracts Nos. PB96-0819 and BFM2000-0806. N.A. acknowledges support from US AROFE (grant N62649-01-1-0002).

References

[1] M. Stich, M. Ipsen, A.S. Mikhailov, Phys. Rev. Lett. 86 (2001) 4406.
[2] P. Kolodner, D. Bensimon, C.M. Surko, Phys. Rev. Lett. 60 (1988) 1723.
[3] A. Mecozzi, J.D. Moores, H.A. Haus, Y. Lai, Opt. Lett. 16 (1991) 1841;
A. Mecozzi, J.D. Moores, H.A. Haus, Y. Lai, J. Opt. Soc. Am. B 9 (1992) 1350.
[4] Y. Kodama, A. Hasegawa, Opt. Lett. 17 (1992) 31.
[5] L.F. Mollenauer, J.P. Gordon, S.G. Evangelides, Opt. Lett. 17 (1992) 1575.
[6] Y. Kodama, M. Romagnoli, S. Wabnitz, Electron. Lett. 28 (1992) 1981.
[7] M. Matsumoto, H. Ikeda, T. Uda, A. Hasegawa, J. Lightwave Technol. 13 (1995) 658.
[8] J.D. Moores, Opt. Commun. 96 (1993) 65.
[9] O.E. Martinez, R.L. Fork, J.P. Gordon, J. Opt. Soc. Am. 2 (1985) 753.
[10] C.-J. Chen, P.K.A. Wai, C.R. Menyuk, Opt. Lett. 19 (1994) 198;
C.-J. Chen, P.K.A. Wai, C.R. Menyuk, Opt. Lett. 20 (1995) 350.
[11] P.A. Belanger, J. Opt. Soc. Am. B 8 (1991) 2077.
[12] H.A. Haus, J.G. Fujimoto, E.P. Ippen, J. Opt. Soc. Am. B 8 (1991) 2068.
[13] M. Hofer, M.E. Fernmann, F. Haberl, M.H. Ober, A.J. Schmidt, Opt. Lett. 16 (1991) 502.
[14] C. De Angelis, M. Santagiustina, S. Wabnitz, Opt. Commun. 122 (1995) 23.
[15] V.B. Taranenko, K. Staliunas, C.O. Weiss, Phys. Rev. Lett. 81 (1998) 2236.
[16] W.J. Firth, A.J. Scroggie, Phys. Rev. Lett. 76 (1996) 1623.
[17] N.A. Kaliteevstii, N.N. Rozanov, S.V. Fedorov, Opt. Spectrosk. 85 (1998) 533.
[18] G.-L. Oppo, G. D'Alessandro, W.J. Firth, Phys. Rev. A 44 (1991) 4712.
[19] D. Michaelis, U. Peschel, F. Lederer, Opt. Lett. 23 (1998) 1814.
[20] N. Akhmediev, A. Ankiewicz, Solitons, Nonlinear Pulses and Beams, Chapman & Hall, 1997.
[21] W. Van Saarloos, P.C. Hohenberg, Physica D 56 (1992) 303.
[22] N.N. Akhmediev, V.V. Afanasjev, J.M. Soto-Crespo, Phys. Rev. E 53 (1996) 1190;
N.N. Akhmediev, V.V. Afanasjev, Phys. Rev. Lett. 75 (1995) 2320.
[23] N. Bekki, K. Nozaki, Phys. Lett. A 110 (1985) 133.
[24] N. Akhmediev, J.M. Soto-Crespo, in: Proc. SPIE, Vol. 3666, 1999, pp. 307–316.
[25] V.V. Afanasjev, N. Akhmediev, J.M. Soto-Crespo, Phys. Rev. E 53 (1996) 1931.
[26] J.M. Soto-Crespo, N. Akhmediev, A. Ankiewicz, Phys. Rev. Lett. 85 (2000) 2937.
[27] V. Hakim, P. Jakobsen, Y. Pomeau, Europhys. Lett. 11 (1990) 19.
[28] S. Fauve, O. Thual, Phys. Rev. Lett. 64 (1990) 282;
O. Thual, S. Fauve, J. Phys. (France) 49 (1988) 1829.
[29] H.R. Brand, R.J. Deisler, Phys. Rev. Lett. 63 (1989) 2801.
[30] J.M. Soto-Crespo, N.N. Akhmediev, V.V. Afanasjev, J. Opt. Soc. Am. B 13 (1996) 1439.
[31] J.M. Soto-Crespo, N.N. Akhmediev, V.V. Afanasjev, S. Wabnitz, Phys. Rev. E 55 (1997) 4783.
[32] N.N. Akhmediev, A. Ankiewicz, J.M. Soto-Crespo, Phys. Rev. Lett. 79 (1997) 4047.
[33] N.N. Akhmediev, A. Ankiewicz, J.M. Soto-Crespo, J. Opt. Soc. Am. B 15 (1998) 515.
[34] T. Kapitula, B. Sandstede, Physica D 124 (1998) 58;
T. Kapitula, B. Sandstede, Physica D 116 (1998) 95.
[35] J.M. Soto-Crespo, D.R. Heatley, E.M. Wright, N.N. Akhmediev, Phys. Rev. A 44 (1991) 636.